Sugiana *et al.*
Asian Journal of Atmospheric Environment (2023) 17:13
https://doi.org/10.1007/s44273-023-00014-9

Asian Journal of Atmospheric Environment

RESEARCH ARTICLE

Open Access

Soil greenhouse gas fluxes to the atmosphere during the wet season across mangrove zones in Benoa Bay, Indonesia

I Putu Sugiana[1,2*], Elok Faiqoh[3], Maria Fernanda Adame[4], Gede Surya Indrawan[3], Anak Agung Eka Andiani[1,2], I Gusti Ayu Istri Pradnyandari Dewi[1,2] and I Wayan Eka Dharmawan[5]

Abstract

Behind their role as carbon sinks, mangrove soil can also emit greenhouse gases (GHG) through microbial metabolism. GHG flux measurments of mangroves are scarce in many locations, including Indonesia, which has one of the world's most extensive and carbon-rich mangrove forests. We measured GHG fluxes (CO_2, CH_4, and N_2O) during the wet season in Benoa Bay, Bali, a bay with considerable anthropogenic pressures. The mangroves of this Bay are dominated by *Rhizophora* and *Sonneratia* spp and have a characteristic zonation pattern. We used closed chambers to measure GHG at the three mangrove zones within three sites. Emissions ranged from 1563.5 to 2644.7 μmol m^{-2} h^{-1} for CO_2, 10.0 to 34.7 μmol m^{-2} h^{-1} for CH_4, and 0.6 to 1.4 μmol m^{-2} h^{-1} for N_2O. All GHG fluxes were not significantly different across zones. However, most of the GHG fluxes decreased landward to seaward. Higher soil organic carbon was associated with larger CO_2 and CH_4 emissions, while lower redox potential and porewater salinity were associated with larger CH_4 emissions. These data suggest that soil characteristics, which are partially determined by location in the intertidal, significantly influence GHG emissions in soils of these mangroves.

Keywords Carbon, Global warming potential, Intertidal, Methane, Nitrous oxide, Wetlands

1 Introduction

The world is facing climate change, causing irregular weather patterns in the past decades. Global climate change is caused by an increase in atmospheric greenhouse gas (GHG) concentrations, including carbon dioxide (CO_2), methane (CH_4), and nitrous oxide (N_2O) (Montzka et al., 2011; Kweku et al., 2018). The CO_2 concentration in the atmosphere has increased to 409.9 ppm since the pre-industrial times (IPCC, 2021), while CH_4 and N_2O have increased by 5–10 and 1 ppb per year, respectively (Reay et al., 2018). Even though CH_4 and N_2O are emitted at lower concentrations, they have an average of a hundred-year global warming effect (100 GWP) of 29.8 and 273 times that of CO_2, respectively (IPCC, 2021).

Mangroves are important sites for carbon accumulation, although their carbon-rich soils can also be sources of GHGs (Alongi, 2014; Chen et al., 2016). Mangrove vegetation fixes CO_2 and stores carbon as aboveground biomass and roots (Bouillon et al., 2008; Murdiyarso et al., 2015), while some of the fixed carbon is exported as litter to adjacent coastal ecosystems

*Correspondence:
I Putu Sugiana
putusugiana@student.unud.ac.id
[1] Bali Research Center, Jl. Gunung Talang VI-C No. 10A, Padangsambian, Denpasar, Bali 80117, Indonesia
[2] Environmental Research Center, Udayana University, Jl. PB. Sudirman, Denpasar, Bali 80234, Indonesia
[3] Department of Marine Science, Udayana University, Jl. Raya Kampus Unud, Badung, Bali 80361, Indonesia
[4] Australian Rivers Institute, Griffith University, Nathan, QLD 4111, Australia
[5] Research Center for Oceanography, National Research and Innovation Agency, Jl. Pasir Putih I, No. 1, North Jakarta, Jakarta 14430, Indonesia

Springer

© The Author(s) 2023. **Open Access** This article is licensed under a Creative Commons Attribution 4.0 International License, which permits use, sharing, adaptation, distribution and reproduction in any medium or format, as long as you give appropriate credit to the original author(s) and the source, provide a link to the Creative Commons licence, and indicate if changes were made. The images or other third party material in this article are included in the article's Creative Commons licence, unless indicated otherwise in a credit line to the material. If material is not included in the article's Creative Commons licence and your intended use is not permitted by statutory regulation or exceeds the permitted use, you will need to obtain permission directly from the copyright holder. To view a copy of this licence, visit http://creativecommons.org/licenses/by/4.0/.

(Adame & Lovelock, 2011). The rest is either decomposed by microorganisms or consumed by animals (Bardgett et al., 2008; Shiau & Chiu, 2020). The decomposition of organic carbon causes CO_2 production in the soil oxic layers and CH_4 production in the anoxic layers (Wang et al., 2009; Treat et al., 2015). Additionally, N_2O is emitted through the nitrogenous pathway involving soil nitrification in the presence of O_2 or denitrification in anoxic conditions, where soil carbon is high and oxygen is low (Zhu et al., 2013; Queiroz et al., 2019).

The GHG emissions in mangrove soils have been associated with environmental factors, including organic carbon, salinity, nutrients, and redox potential (Chen et al., 2010, 2014; Welti et al., 2017). GHG emissions increase with nutrient inputs and soil organic carbon (Chen et al., 2010, 2014) and decrease with salinity (Chen et al., 2010). For instance, CH_4 is more likely to be produced under low-salinity conditions due to reduced competition with sulfate- and nitrate-reducing bacteria, which are more energy efficient than methanogenic bacteria (Purvaja & Ramesh, 2001; Biswas et al., 2007).

Mangroves exhibit zoning patterns across the intertidal area with characteristic redox and salinity gradients (Naidoo, 2016; Srikanth et al., 2016), which are likely to influence GHG emissions (Ulumuddin, 2019). Mangrove species with solid root structures, such as *Sonneratia* and *Rhizophora*, tend to dominate in the seaward or fringing forest (Tomlinson, 2016), where flooding is frequent, salinity is more less constant, and nutrient inputs are high (Ulumuddin, 2019). Variability across the intertidal zone also drives soil microorganism occurrence and metabolism, both of which are closely associated with GHG production (Chen et al., 2014). Other factors are also likely to affect mangrove characteristics and biogeochemical processes, such as climate and geomorphology (Lugo & Snedakers, 1974; Shih & Cheng, 2022), but at the local scale, mangrove zonation is likely to be one of the most important factors.

Measurements on GHG emissions in mangrove soils in many countries have been limited (Sasmito et al., 2019), including in Indonesia (Chen et al., 2014; Cameron et al., 2019; Sidik et al., 2019). Indonesia has one of the largest mangrove areas in the world, accounting for 19.5% of the total (Bunting et al., 2018). Indonesia has also one of the highest rates of mangrove loss (Richards & Friess, 2016), which are causing substantial GHG emissions (Maiti & Chowdhury, 2013). Thus, Indonesia has a high potential to reduce its emissions by reducing deforestation and supporting mangrove restoration (Buelow et al., 2022). However, to accurately estimate the carbon gains from mangrove protection and restoration, the baseline GHG emissions need to be excluded from their carbon mitigation potential (Rosentreter et al., 2021).

Indonesia is a tropical archipelagic country which a large variety of mangrove ecosystems, which are globally significant for its blue carbon and multiple co-benefits (Murdiyarso et al., 2015). Indonesia's estuaries have significant freshwater inputs forming characteristic salinity gradients, which drive different types of mangrove species composition and structure, thus likely highly variable GHG emissions. One mangrove ecosystem experiencing high anthropogenic pressure is Benoa Bay in Bali. The Bay suffers from nutrient pollution (Raharja et al., 2018; Rahayu et al., 2018) and massive sedimentation caused by land reclamation, which has already caused the deterioration of the mangroves. Thus, this site is urgently needed for management and restoration activities, potentially through Blue Carbon projects.

The objectives of this study were as follows: first, to estimate the GHG fluxes (CO_2, CH_4, and N_2O) in the mangroves of Benoa Bay along the intertidal zone (seaward, middle, and landward) and, second, to assess the relationship between GHG fluxes, forest structure, and environmental parameters (salinity, oxidation reduction potential, soil organic carbon). The wet or rainy season was chosen as the sampling time due to the maximum potential for soil GHG fluxes in tropical mangrove forests to occur (Kristensen et al., 2008; Tang et al., 2018; Otero et al., 2020; Kitpakornsanti et al., 2022). The main goal was to provide baseline data from these human-impacted mangroves in Indonesia. The result from this study will support the Indonesian government program *FoLU (Forestry and Other Land Use) Net Sink 2030* by providing GHG fluxes data from the forestry sector. This information can be useful to accurately assess the carbon sequestration capacity and potential for reduced emissions of mangroves they are appropriately managed. We hypothesized that GHG fluxes during wet season will differ among mangrove community zones due to differences in vegetation structure and environmental conditions along the intertidal zone.

2 Methods

2.1 Site description

Benoa Bay, Bali (8°43′ to 8°42′S, 115°11′ to115°14′W; Fig. 1), has a large area of mangrove forest with 1132 ha. The mangroves have distinct zonation patterns, starting from the sea zone (seaward), which is dominated by *Sonneratia alba*, continuing to the middle zone, which is dominated by *Rhizophora* spp. and the landward zone, which has mixed mangrove species (Andiani et al., 2021; Sugiana et al., 2022). Seaward and middle zones are frequently flooded during high tides, while the landward zone is only inundated during large spring tides (Fig. 1).

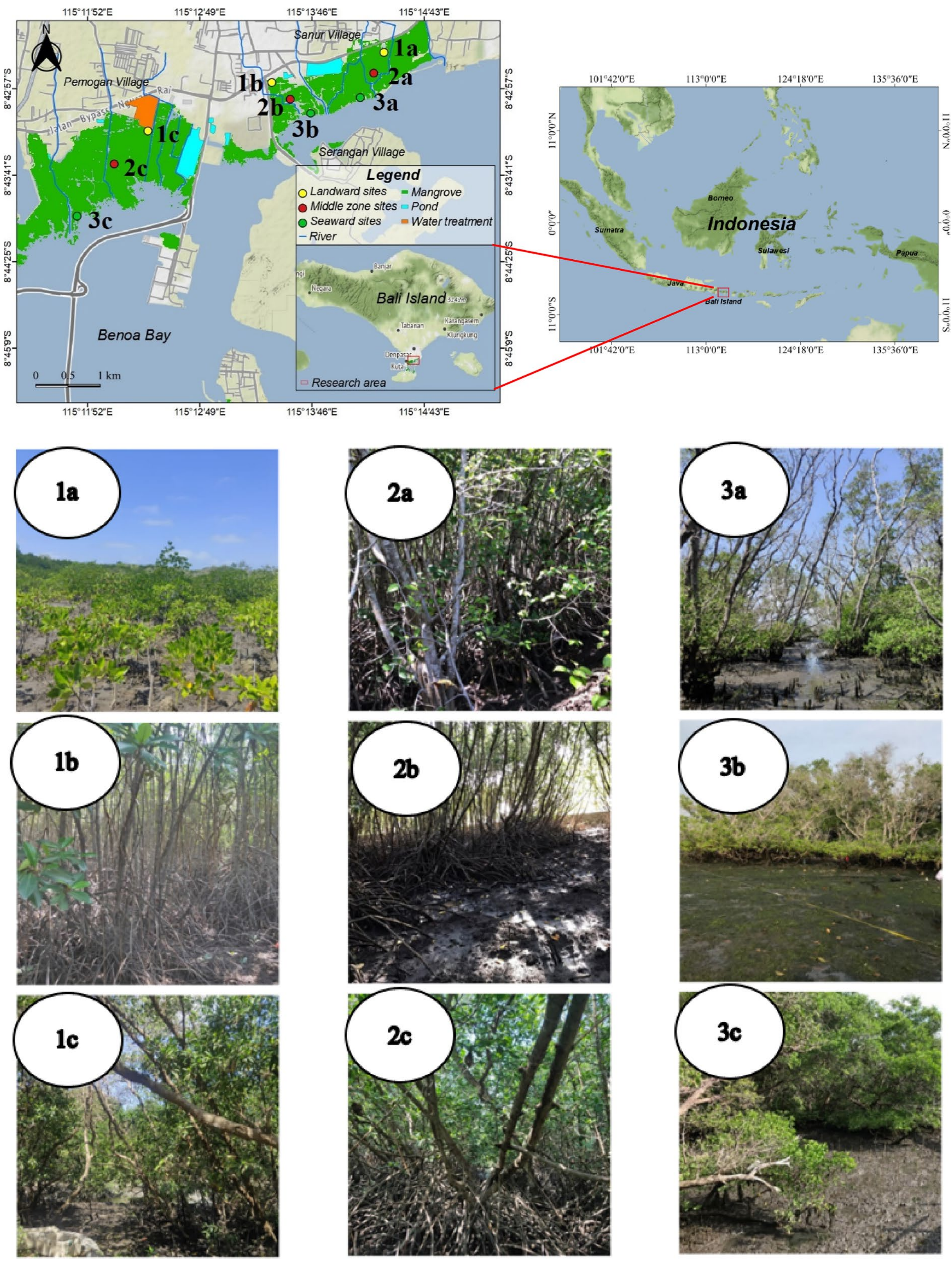

Fig. 1 Study sites in Benoa Bay, Bali, Indonesia. 1 Landward plots, 2 middle plots, and 3 seaward plots

The soil texture ranges from fine sand to gravel but is dominated by coarse sand (Imamsyah et al., 2020; Prinasti et al., 2020). The porewater salinity of these mangroves generally increases, while the redox decreases, from the land to the seaward edge (Sugiana et al., 2021).

We sampled nine plots within three forests close to three villages: Sanur, Serangan, and Pemogan, during the wet season at low tide of the new moon period (3–9 December 2021) at daylight (1 pm–3 pm; UTC + 8). During sampling, temperatures ranged from 23.2 to 34.6 °C (average: 30.1 °C), humidity levels ranged from 58.0 to 98.0% (average: 76.4%), and monthly rainfall was 549.0 mm (Denpasar Central Statistics Agency, 2022).

2.2 Greenhouse gas flux measurement

We used the closed chamber method adopted from Chen et al. (2016). At each plot, three 20 × 20 × 25 cm squared dark chambers were installed at 2 cm deep in the soil. Gas samples were collected using 10-mL syringes plot for 30 min at 10-min intervals (0, 10, 20, 30 min for total 108 samples). We only took the gas once on each plot due to access difficulties and the limitation of low tide time, which only lasted for 2 h, especially on the seaward edge. The GHG concentrations were analyzed with gas chromatography (450-GC Varian) equipped with a flame ionization detector (FID), a thermal conductivity detector (TCD), and a ^{63}Ni electron capture detector (μECD) for CH_4, CO_2, and N_2O consecutively. The 450-GC also has a PAL autosampler injector, which functions for auto-injection and uses Ar, H_2, He, N_2, and compressed air as carrier gas. The measurement process began at under 25 °C at room temperature. A standard curve was used as a reference in the analysis. The concentration of GHG was calculated by comparing the peak area of the sample with the standard curve. The relationships between deployment time and GHG concentrations were significant (R^2 of 0.83–0.98, 0.76–0.94, and 0.79–0.94 for CO_2, CH_4, and N_2O, respectively, Fig. 2), thus confirming that the mangrove sediment continuously resealed gases that were accumulated in the chambers during sampling. The GHG fluxes were calculated as in Chen et al. (2016):

$$Fm = \frac{V\,x\,\Delta M\,x\,10^6}{A\,x\,P}$$

where

Fm: GHG fluxes (μmol m^{-2} h^{-1})

ΔM: The slope of the linear regression line between GHG concentrations (ppm) and sampling frequency (10 min transformed to an hour)

V: Chamber volume (L)

A: Chamber area (m^2)

P: Constant gas volume (m^3 mol^{-1})

Based on the average gas fluxes of the three mangrove zones, the CH_4 and N_2O fluxes were converted to CO_2-equivalent fluxes to indicate the gas warming effect (IPCC, 2021). The CO_2-equivalent flux was calculated using the following formula:

$$Fe = Fm\,x\,M\,x\,GMP$$

where

Fe: CO_2-equivalent flux (g CO_2 m^{-2} h^{-1}),

Fm: Interfacial gas flux (mol m^{-2} h^{-1})

M: Molecular weight of the GHG

GMP: Warming effect or the conversion of CH_4 and N_2O emissions to CO_2 equivalents as 29.8 and 273, respectively, over a 100-year timeframe (IPCC, 2021).

2.3 Soil and porewater physicochemical characteristics

Temperature, pH, salinity, and oxidation reduction potential (ORP) in the water and sediment were measured during sampling with a pH meter EZODOPH5011, SCT meter YSI EC200, and multimeter COM-600 water quality tester. Soil samples were collected from each plot at a depth of 5 cm using a 10-cm-diameter core pipe, from which water content and soil organic carbon (SOC) were measured. Samples were dried at 70 °C until constant weight and reweighed to measure water content. For SOC, the soil was filtered through a 2-mm mesh and burned at 550° (Chen et al., 2014). Soil type was identified with the megascopic method and the Wentworth diagram (1922).

2.4 Forest structure

Forest structure was measured following the guidelines from COREMAP-CTI LIPI (Dharmawan et al., 2020). At each site, we measured tree and sapling density, canopy coverage, and diameter at breast height (DBH) within a 10 × 10 m plot. Each plant was classified either as a tree ($DBH \geq 5$ cm) or a sapling ($DBH < 5$ cm), and its species was identified based on Giesen et al. (2007) and Tomlinson (2016). Density, dominance, and species were used to estimate the importance value index (IVI). Field data collection was run in the MonMang 2.0 application, similar to Sugiana et al. (2022).

Hemispherical photography was used to estimate mangrove canopy coverage in each zone (Jennings et al., 1999; Ishida, 2004). Squared output hemisphere photographs were captured from scattered positions on each plot using a smartphone with 16-MP resolution. Each photograph was analyzed using ImageJ software to count the number of pixels. Canopy coverage percentage was calculated by comparing the number of pixels with vegetation to the total number of pixels on each photograph. The mangrove health index (MHI) was calculated

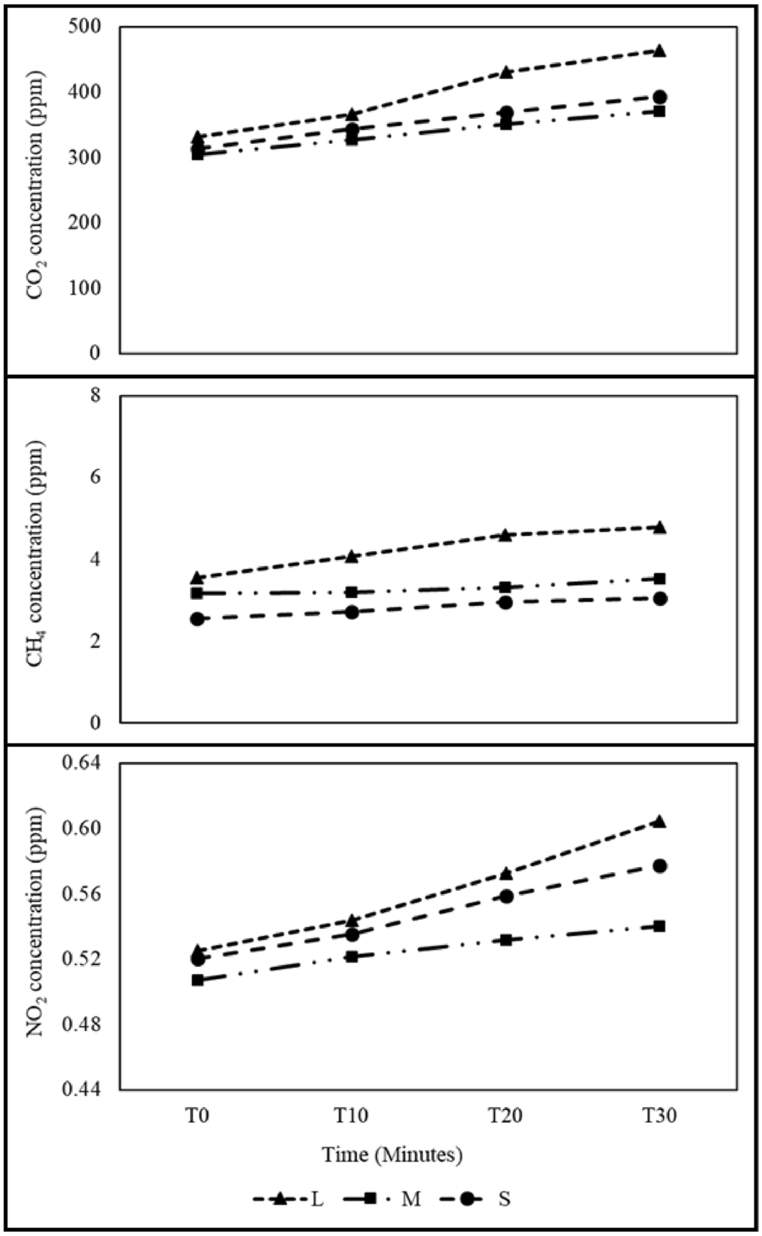

Fig. 2 The trend between GHG concentrations and deployment times for each mangrove zone

by combining data on canopy cover, density, and DBH (Dharmawan & Ulumuddin, 2021), and below-ground carbon (BGC) is also measured by converting DBH of each mangrove stands using allometric equation based on Kauffman and Donato (2012).

2.5 Statistical analyses

All univariate data were analyzed with the Shapiro-Wilk normality test. Environmental parameters were normally distributed ($p > 0.05$) and were compared against zones with an analysis of variance (ANOVA) and Tukey HSD test for each mangrove zone. The GHG flux data were not normally distributed ($p < 0.05$), hence were analyzed with the nonparametric Kruskal-Wallis and Spearman rank. The GHG emissions were compared among zones and against environmental parameters (forest structure, soil, and porewater properties). All the tests used a statistical level of $p < 0.05$ and were run with the R software version 4.0.2.

3 Results

3.1 Forest structure

Species composition was different among mangrove zones, with the landward zone being the most diverse, with six mangrove spp. dominated by *Sonneratia alba* ($IVI=107.1\%$). The middle zone had two mangrove species dominated by *Rhizophora apiculata* ($IVI=175.1\%$, Table 1), and the seaward zone was solely composed of *S. alba* ($IVI=300.0\%$). A significantly higher density of mangrove trees and saplings was found in the middle zone with 3900 ± 1654 tree ha^{-1} (ANOVA: $F_{3.6}=4.67$, $p<0.05$) and 1400 ± 1015 tree ha^{-1} (ANOVA: $F_{3.6}=5.52$, $p<0.05$), respectively, compared to the land and seaward zone. The seaward zone had higher DBH (13.6 ± 1.7 cm) and lower canopy cover (40.8 ± 14.3%) compared to the land and middle zones 7.9 ± 3.1 cm and 7.8 ± 0.9 cm (ANOVA: $F_{3.6}=22.38$, $p<0.05$) and 72.9 ± 5.7% and 78.7 ± 1.1%, respectively (ANOVA: $F_{3.6}=47.30$, $p<0.05$), respectively. Even though the seaward zone had the largest DBH, it had the lowest MHI values with 41.0 ± 3.0% compared to land and middle zones with 51.2 ± 5.7% and 58.0 ± 3.6% (ANOVA: $F_{3.6}=36.57$, $p<0.05$), respectively. The low MHI value in the seaward zone was caused by its low canopy cover and sapling density. Despite the significant difference among the MHI across zones ($p<0.05$, Table 1), they were all in the same category, suggesting a "moderate" condition. Below-ground carbon (BGC) from mangrove roots was also significantly different between the middle zone and the other two zones ($F_{3.6}=40.19$, $p<0.05$), with the higest value found in middle zone at 229.5 ± 84.4 Mg ha^{-1}.

3.2 Soil and porewater physicochemical characteristics

The mangrove soil was mainly mud, except for the seaward zone, which was composed of sand and mud (Table 2). Water content during sampling was significantly highest in the middle zone with 50.9 ± 7.5% (ANOVA: $F_{3.6}=29.83$, $p<0.05$), and SOC concentrations were similar among zones ($F_{3.6}=0.80$, $p>0.05$), with values ranging from 19.8 to 25.8 mg g^{-1}. The temperature

Table 1 Mangrove community parameters across the landward, middle, and seaward zones

Parameter	Zone		
	Landward	**Middle**	**Seaward**
Dominance of mangrove spp.	***Sonneratia alba* (IVI: 107.1%)**	***Rhizophora apiculata* (IVI: 175.1%)**	***Sonneratia alba* (IVI: 300.0%)**
Number of spp.	6	2	1
Tree density (stands ha^{-1})	2400 ± 2063^{ab}	3900 ± 1654^{a}	1600 ± 966^{b}
Sapling density (stands ha^{-1})	900 ± 772^{ab}	1400 ± 1015^{a}	200 ± 205^{b}
Diameter at breast height (cm)	7.9 ± 3.1^{a}	7.8 ± 0.9^{a}	13.6 ± 1.7^{b}
Canopy coverage (%)	72.9 ± 78.7^{a}	78.7 ± 1.1^{a}	40.8 ± 14.3^{b}
Mangrove health index (%)	51.2 ± 5.7^{a}	58.0 ± 3.6^{b}	41.0 ± 3.0^{c}
BGC (root) (Mg ha^{-1})	26.5 ± 20.7^{a}	229.5 ± 84.4^{b}	48.4 ± 28.3^{a}

Superscript letters depict significant differences among zones ($p<0.05$)

Table 2 Mangrove soil and porewater physicochemical properties across the landward, middle, and seaward zones

Parameter	Zone		
	Landward	**Middle**	**Seaward**
Soil			
Soil characteristics	Muddy	Muddy	Sandy mud
Water content (%)	36.81 ± 6.51^{a}	50.88 ± 7.48^{b}	28.00 ± 4.72^{c}
Organic carbon (mg g^{-1})	25.53 ± 17.38^{a}	25.80 ± 6.73^{a}	19.84 ± 5.85^{a}
Porewater			
Temperature (℃)	29.8 ± 1.4^{a}	29.9 ± 1.0^{a}	30.4 ± 2.2^{a}
pH	6.58 ± 0.24^{a}	6.60 ± 0.10^{a}	7.04 ± 0.12^{b}
Salinity (ppt)	26.30 ± 2.44^{ab}	24.03 ± 2.24^{a}	28.26 ± 1.34^{b}
Oxidation reduction potential (mV)	-108.2 ± 71.5^{a}	-20.2 ± 71.5^{ab}	21.1 ± 83.5^{b}

Superscript letters depict significant differences among zones ($p<0.05$)

of the porewater was similar among zones, with a mean value of 30.4 °C (ANOVA: $F_{3.6} = 0.38$, $p > 0.05$). Water pH, salinity, and ORP were significantly different in the seaward compared to the rest of the zones with mean values of 7.0 ± 0.1 (ANOVA: $F_{3.6} = 23.29$, $p < 0.05$), 28.3 ± 1.3 ppt (ANOVA: $F_{3.6} = 8.40$, $p < 0.05$), and 21.1 ± 82.8 mV (ANOVA: $F_{3.6} = 6.85$, $p < 0.05$) as can be seen in Table 2.

3.3 Greenhouse gas fluxes

The CO_2 emissions were similar among mangrove zones (K-Wallis: $H_{3,6} = 0.03$, $p > 0.05$), although with a trend of

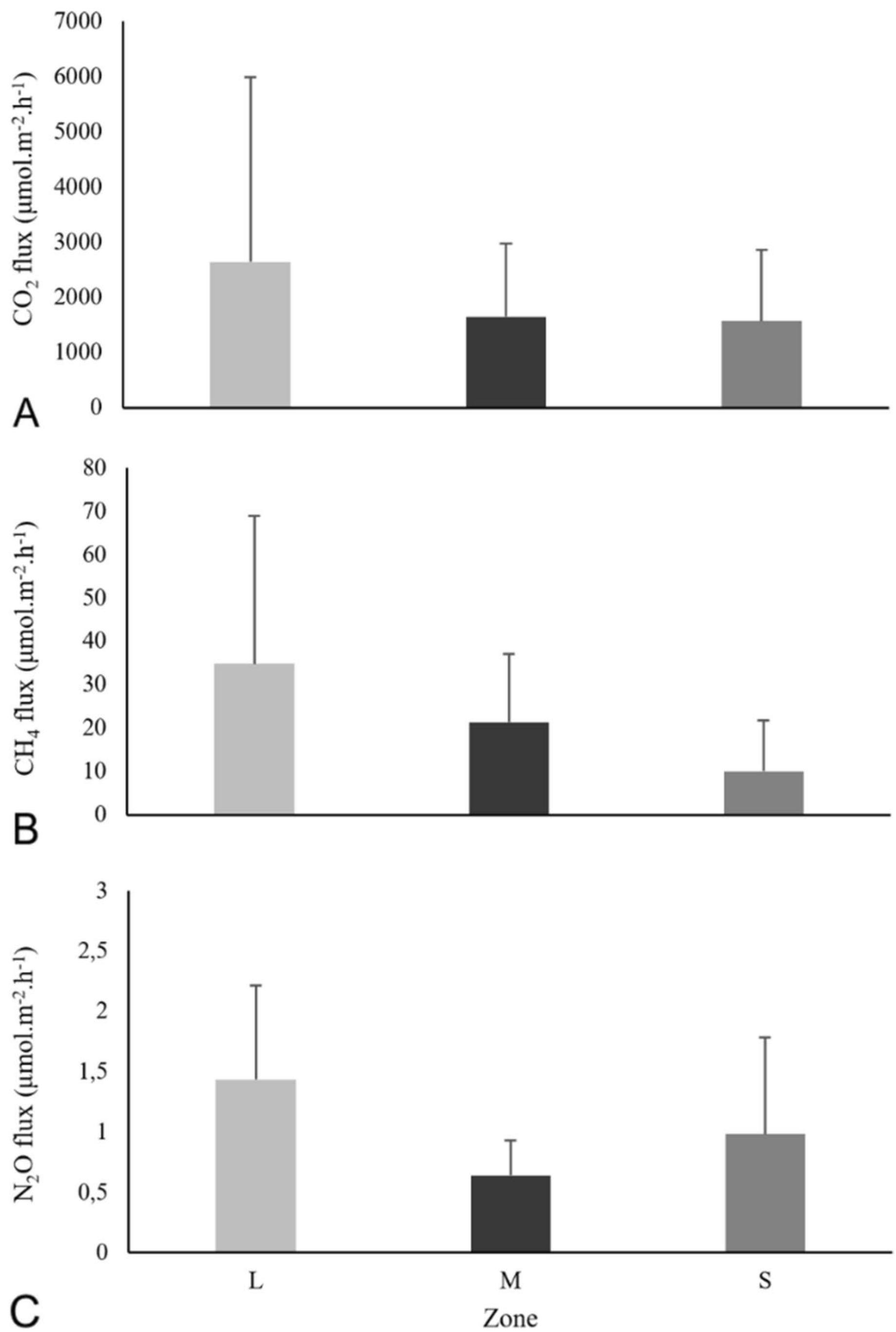

Fig. 3 **A** CO_2, **B** CH_4, and **C** N_2O fluxes (μmol m^{-2} h^{-1}) from mangrove soils in the landward (L), middle (M), and seaward (S) zone in Benoa Bay, Indonesia

decreasing emissions from the land (2,644.7 ± 3,338.8; range of 314.8 to 8,952.8 μmol m^{-2} h^{-1}) to the middle (1,646.6 ± 1,335.6; 266.1 to 4,175.4 μmol m^{-2} h^{-1}) and the seaward zone (1,563.5 ± 1,302.4; 97.8 to 3,578.3 μmol m^{-2} h^{-1}; Fig. 3A). Similarly, CH_4 and N_2O flux patterns tended to decrease from the land to the sea, although the differences were not significant (CH_4 K-Wallis: $H_{3.6}=5.89$, $p>0.05$ and N_2O K-Wallis $H_{3.6}=5.04$, $p>0.05$). The CH_4 flux in the landward zone was 34.7 ± 34.1 (5.0 to 88.0) μmol m^{-2} h^{-1}, the middle zone was 21.36 ± 15.72 (5.0 to 44.4) μmol m^{-2} h^{-1}, while the seaward zone was 10.0 ± 11.7 (0.9 to 38.5) μmol m^{-2} h^{-1} (Fig. 3B). For N_2O, the landward flux was 1.4 ± 0.8 (0.43 to 2.96) μmol m^{-2} h^{-1}, followed by the middle zone with 1.0 ± 0.8 (0.35 to 3.60) μmol m^{-2} h^{-1}, and, finally, the seaward zone with 0.6 ± 0.3 (0.2 to 1.5) μmol m^{-2} h^{-1} (Fig. 3C). The CO_2-equivalent fluxes from CH_4 and N_2O showed a similar decreasing trend from the land to the sea with a total mean GWP of 19.2 mg CO_2 m^{-2} h^{-1} (Table 3).

3.4 Correlation with environmental parameters

Soil parameters were positively correlated with CO_2 and CH_4, but not with N_2O fluxes. Higher soil organic carbon was associated with larger CO_2 ($p=1.9\times10^{-2}$) and CH_4 fluxes ($p=5\times10^{-4}$), while lower ORP and low porewater salinity were associated with larger CH_4 fluxes ($p=2.3\times10^{-2}$ and 2.9×10^{-3}, respectively). Forest structure parameters were not significantly correlated with GHG fluxes (Table 4).

4 Discussion

The GHG fluxes in mangroves from Benoa Bay, Indonesia, had a decreasing trend from the land to the seaward zone. The CO_2 and CH_4 fluxes were significantly higher where SOC was highest, and CH_4 flux were significantly highest where salinity and ORP were lowest. These results complement current literature showing that soil physicochemical characteristics are important drivers of GHG emissions in mangroves (Chen et al., 2010). Our results also prove that in addition to sequestering carbon, pollution-impacted mangroves release GHG from sediments, which need to be accounted for when estimating their full carbon mitigation potential.

Other studies have shown significant changes in GHG fluxes across intertidal zones, some finding higher emissions in the seaward (Wang et al., 2009) and others in the landward zone (Hirota et al., 2007; Chen et al., 2010; Lin et al., 2020). Each mangrove zone has unique vegetation characteristics, resulting mainly from tidal inundation variations, which drive interstitial salinity and nutrient availability. Similarly, in Benoa Bay, mangrove structure is quite different among zones, including the density of trees and saplings, the size of tree trunks, and the canopy cover. Additionally, pH was also significantly different among zones. Despite showing different values among zones, none of these parameters was significantly associated with GHG fluxes, suggesting that the effect of forest structure and pH was a less strong predictor than SOC and salinity. However, SOC was also influenced by vegetation density, where the denser the vegetation, the higher the carbon stores in the soil. However, this statement should be further studied, considering its weak relationship, and only applied if the measured vegetation density comes from the same species (Dermawan et al., 2023). Each vegetation species has a different contribution to the burial rate of SOC (Weiss et al., 2016), so this needs to be considered since SOC was closely correlated to GHG fluxes.

Table 3 CO_2-equivalent greenhouse gas fluxes from mangrove soils within the intertidal zones in Benoa Bay, Indonesia

Zone	CO_2-equivalent flux (mg CO_2 m^{-2} h^{-1})	
	CH_4	N_2O
Landwards	11.2	17.0
Middle	6.9	7.7
Seawards	3.2	11.7
Average	7.1	12.1

Table 4 Spearman-rank correlation coefficient values (*r*) among soil, porewater and mangrove structure, and greenhouse gases

Parameter	Correlation coefficient		
	CO_2	CH_4	N_2O
Soil			
Water content (%)	0.18	0.30	−0.05
Organic carbon (mg g^{-1})	0.45*	0.63**	−0.08
Porewater			
Temperature (°C)	0.19	0.01	−0.08
pH	−0.11	−0.20	−0.27
Salinity (ppt)	−0.13	−0.55**	−0.02
Oxidation reduction potential (mV)	−0.11	−0.44*	−0.29
Mangrove structure			
Tree density (tree ha^{-1})	−0.10	0.20	−0.27
Sapling density (sapling ha^{-1})	−0.24	0.01	0.07
Diameter (cm)	0.15	−0.14	−0.12
Canopy coverage (%)	0.19	0.36	−0.09
Mangrove health index (%)	0.16	0.31	−0.03
Belowground Carbon (roots) (Mg ha^{-1})	0.05	0.09	−0.34

* and ** indicate significant *r*-value at $p<0.05$ and 0.01, respectively ($n=27$)

Table 5 Comparison of GHG fluxes in mangroves soil of Benoa Bay with other tropical and subtropical regions

Location	Area	CO_2 fluxes (μmol $m^{-2} h^{-1}$)	CH_4 fluxes (μmol $m^{-2} h^{-1}$)	N_2O fluxes (μmol $m^{-2} h^{-1}$)	Reference
Benoa Bay, Bali	Tropical	98–8953	0.9–88.0	0.24–3.6	This study
Budai, Taiwan	Sub-tropical	NA	14.1–316.9	NA	Lin et al. (2020)
Bhitarkanika, India	Sub-tropical	NA	5	0.20	Chauhan et al. (2015)
Sulawesi, Indonesia	Tropical	−1340–3880	−6.1–13.1	−0.35–0.61	Chen et al. (2014)
Maipo, Hongkong	Sub-tropical	31	NA	11.6	Chen et al. (2012)
Futian, China	Sub-tropical	560–20.6	10.1–5168.6	0.14–23.8	Chen et al. (2010)
Brisbane, Australia	Sub-tropical	NA	272.5	40.4	Allen et al. (2007)

NA Not available

In Benoa Bay, the heterogeneous structure of the mangrove forest has caused differences in stand structure, such as the seaward zone, which is dominated by *Sonneratia alba*, with lower stand density due to its allelopathic compounds (Li et al., 2015; Zhang et al., 2018), compared to the middle zone, which is dominated by *Rhizophora apiculata*. Apart from SOC burial contribution, variations in mangrove species also indicate differences in salinity. *Sonneratia alba* could tolerate high water salinity, which makes this species dominate the seaward zone with more frequent seawater input (Pillai & Harilal, 2016). In addition, due to the more frequent washing of seawater through tides, SOC concentrations in the seaward zone tend to be lower than in the other zones. Therefore, differences in the zoning pattern of mangrove forests also indirectly indicate variations in GHG fluxes.

The higher fluxes at higher SOC make sense, as a higher carbon source for soil microorganisms results in higher rates of anoxic and anaerobic respiration (Bouillon et al., 2008; Morell et al., 2011). Similar results were found in South China (Chen et al., 2010) and Jiulong River estuary, China (Chen et al., 2016), where a positive correlation between SOC with CO_2 and CH_4 fluxes was found. Organic carbon sources in sediments come from within or outside the mangrove ecosystem, such as anthropogenic carbon carried by rivers or tides (Ulumuddin, 2019). Decomposition and respiration of organic carbon in mangrove soils result in CO_2 or CH_4 fluxes; however, the proportion of these gases depends on environmental conditions within the mangrove soil.

The CH_4 fluxes were significantly correlated with low porewater salinity and ORP. Most mangrove soils have soils low in oxygen (Lu et al., 1999; Arai et al., 2016). However, in highly impacted mangroves, where carbon pollution is significant, anoxic conditions favor the production of CH_4 through methanogenesis (Maltby et al., 2016; Sánchez-Carrillo et al., 2021). CH_4 emissions are low in sites with high inputs of marine water, which favors sulfate-reducing bacteria that outcompete methanogens (Ulumuddin, 2019). Although N_2O emissions followed a similar trend as CO_2 and CH_4, these differences were insignificant. Nevertheless, the decreasing N_2O land-seaward trend is expected, as denitrification a likely source of N_2O) is higher where soil organic carbon is high and pH is neutral, which sometimes can occur in the seaward zone (Fernandes et al., 2010; Marton et al., 2012).

Compared to other studies, our results are within the range of other tropical and subtropical regions (Table 5). We acknowledge that our sampling was limited in time; however, the wet season in Benoa Bay is where precipitation and temperature are highest; thus, our data could be representative of the higher end of annual emissions. In addition, these results were also supported by some literature which finds that the wet season becomes the peak of GHG flux in tropical mangrove forests such as CO_2, CH_4, and N_2O in Thailand (Kitpakornsanti et al., 2022); CO_2 in Tanzania and Brazil (Kristensen et al., 2008; Castellón et al., 2021); CH_4 in Malaysia, Brazil, and Myanmar (Tang et al., 2018; Dalmagro et al., 2019; Cameron et al., 2021); and N_2O in Brazil (Otero et al., 2020). In subtropical regions, similar results were also found for CH_4 (Philipp et al., 2017; Zhu et al., 2021). Therefore, if this holds true, CH_4 and N_2O GWP of mangroves in Benoa Bay is about 1.7 $MgCO_2$ ha^{-1} $year^{-1}$, which is lower than CO_2 GWP on natural riverine mangroves in Perancak, Indonesia, with 12.2 $MgCO_2$ ha^{-1} $year^{-1}$ (Sidik et al., 2019) and of rehabilitated mangroves in Sulawesi, Indonesia, with overall GWP of 17 $MgCO_2$ ha^{-1} $year^{-1}$ (Cameron et al., 2019). However, the emission of mangrove soils is low compared to their potential for carbon sequestration, which is estimated at 52.9 $MgCO_2$ ha^{-1} $year^{-1}$ (LIPI, 2018). Thus, regardless of their soil emissions, even in pollution-impacted regions, mangroves still maintain a capacity to mitigate carbon emissions. This result is particularly important given the high national deforestation rate of mangrove forests in Indonesia, which reached 182,091 ha, contributing to 136.9 $MgCO_2$ ha^{-1} $year^{-1}$ (Arifanti et al., 2021). Thus, restoration of mangroves such as those in Benoa Bay could contribute to lowering emissions in Indonesia.

5 Conclusion

GHG emissions in mangroves in Bali slightly varied across mangrove zones, with a decreasing land-to-seaward trend. The main parameters that controlled the emissions were salinity and SOC. Despite the GHG emissions at their maximum value during wet season, mangroves in Benoa Bay are still likely to remove and store significant quantities of carbon. Our data contribute to accurately estimating the carbon mitigation of mangroves in Indonesia. The low GHG emissions in these mangroves support the idea that even disturbed mangroves have potential to act as a carbon sinks. Further monitoring throughout the year could improve our results and identify additional drivers of GHG emissions in Indonesian mangroves and better ways to manage and protect these valuable ecosystems.

Acknowledgements
The authors thank Dr. Bruce Campbell for his constructive criticism during the manuscript preparation and two anonymous reviewers who provided very useful input in improving the quality of this paper. We also thank our Udayana friends, N. P. P. Megasari, N. L. P. B. Witariani, G. A. I. Indrayanti, N. K. A. Safitri, I. M. Yunarta, and P. Kumayarasa for their help during field data collection. This research is a collaboration between Udayana University and the Indonesian National Research and Innovation Agency (BRIN) through BioVeLa (Marine Biovegetation) project.

Authors' contributions
Conceptualization, IPS; methodology, EF, MFA, and GSI; formal analysis and investigation, AAEA, IGAIPD, and GSI; writing — original draft preparation, IPS, MFA, AAEA, and IGAIPD; writing — review and editing, IPS, MFA, and IWED; funding acquisition, IPS, EF, MFA, IWED; resources, IPS, AAEA, IGAIPD; and supervision, MFA and IWED.

Funding
There is no special funding provided during the research.

Availability of data and materials
We are pleased to be able to share the results of the analysis we have. However, we cannot provide all the data due to its use for the ongoing study. The datasets can be accessed at https://docs.google.com/spreadsheets/d/1bf_RCrUTM9ZJsTTgDcT_0JhE100l-dKftFgZ34lYAtw/edit?usp=sharing.

Declarations

Competing interests
The authors declare that they have no competing interests.

Received: 31 May 2023 Accepted: 25 September 2023
Published online: 10 October 2023

References

Adame, M. F., & Lovelock, C. E. (2011). Carbon and nutrient exchange of mangrove forests with the coastal ocean. *Hydrobiologia*, *663*, 23–50. https://doi.org/10.1007/s10750-010-0554-7

Allen, D. E., Dalal, R. C., Rennenberg, H., Meyer, R. L., Reeves, S., & Schmidt, S. (2007). Spatial and temporal variation of nitrous oxide and methane flux between subtropical mangrove sediments and the atmosphere. *Soil Biology and Biochemistry*, *39*(2), 622–631. https://doi.org/10.1016/j.soilbio.2006.09.013

Alongi, D. M. (2014). Carbon cycling and storage in mangrove forests. *Annual Review of Marine Science*, *6*, 195–219. https://doi.org/10.1146/annurev-marine-010213-135020

Andiani, A. A. E., Karang, I. W. G. A., Putra, I. N. G., & Dharmawan, I. W. E. (2021). Relationship among mangrove stand structure parameters in estimating the community scale of aboveground carbon stock. *Journal of Marine Science and Technology*, *13*(3), 485–498. https://doi.org/10.29244/jitkt.v13i3.36363

Arai, H., Yoshioka, R., Hanazawa, S., Minh, V. Q., Tuan, V. Q., Tinh, T. K., Phu, T. Q., Jha, C. S., Rodda, S. R., Dadhwal, V. K., Mano, M., & Inubushi, K. (2016). Function of the methanogenic community in mangrove soils as influenced by the chemical properties of the hydrosphere. *Soil Science and Plant Nutrition*, *62*(2), 150–163. https://doi.org/10.1080/00380768.2016.1165598

Arifanti, V. B., Novita, N., & Tosiani, A. (2021). Mangrove deforestation and CO_2 emissions in Indonesia. *IOP Conference Series: Earth and Environmental Science*, *874*(1), 012006. https://doi.org/10.1088/1755-1315/874/1/012006

Bardgett, R. D., Freeman, C., & Ostle, N. J. (2008). Microbial contributions to climate change through carbon cycle feedbacks. *The ISME Journal*, *2*(8), 805–814. https://doi.org/10.1038/ismej.2008.58

Biswas, H., Mukhopadhyay, S. K., Sen, S., & Jana, T. K. (2007). Spatial and temporal patterns of methane dynamics in the tropical mangrove dominated estuary, NE coast of Bay of Bengal, India. *Journal of Marine Systems*, *68*(1–2), 55–64. https://doi.org/10.1016/j.jmarsys.2006.11.001

Bouillon, S., Borges, A. V., Castañeda-Moya, E., Diele, K., Dittmar, T., Duke, N. C., Kristensen, E., Lee, S. Y., Marchand, C., Middelburg, J. J., Rivera-Monroy, V. H., Smith, T. J. S., III., & Twilley, R. R. (2008). Mangrove production and carbon sinks: A revision of global budget estimates. *Global Biogeochemical Cycles*, *22*(2), 1–12. https://doi.org/10.1029/2007GB003052

Buelow, C. A., Connolly, R. M., Turschwell, M. P., Adame, M. F., Ahmadia, G. N., Andradi-Brown, D. A., Bunting, P., Canty, S. W. J., Dunic, J. C., Friess, D. A., Lee, S. Y., Lovelock, C. E., McClure, E. C., Pearson, R. M., Sievers, M., Sousa, A. I., Worthington, T. A., & Brown, C. J. (2022). Ambitious global targets for mangrove and seagrass recovery. *Current Biology*, *32*(7), 1641–1649. https://doi.org/10.1016/j.cub.2022.02.013

Bunting, P., Rosenqvist, A., Lucas, R. M., Rebelo, L. M., Hilarides, L., Thomas, N., Hardy, A., Itoh, T., Shimada, M., & Finlayson, C. M. (2018). The global mangrove watch—A new 2010 global baseline of mangrove extent. *Remote Sensing*, *10*(10), 1669. https://doi.org/10.3390/rs10101669

Cameron, C., Hutley, L. B., Friess, D. A., & Brown, B. (2019). High greenhouse gas emissions mitigation benefits from mangrove rehabilitation in Sulawesi, Indonesia. *Ecosystem Services*, *40*, 101035. https://doi.org/10.1016/j.ecoser.2019.101035

Cameron, C., Hutley, L. B., Munksgaard, N. C., Phan, S., Aung, T., Thinn, T., Aye, W. M., & Lovelock, C. E. (2021). Impact of an extreme monsoon on CO_2 and CH_4 fluxes from mangrove soils of the Ayeyarwady Delta, Myanmar. *Science of the Total Environment*, *760*, 143422. https://doi.org/10.1016/j.scitotenv.2020.143422

Castellón, S. E. M., Cattanio, J. H., & Berrêdo, J. F. (2021). Spatial and temporal variability of carbon dioxide and methane fluxes in an Amazonian estuary. *International Journal of Hydrology*, *5*(6), 327–337. https://doi.org/10.15406/ijh.2021.05.00294

Chauhan, R., Datta, A., Ramanathan, A. L., & Adhya, T. K. (2015). Factors influencing spatio-temporal variation of methane and nitrous oxide emission from a tropical mangrove of eastern coast of India. *Atmospheric Environment*, *107*, 95–106. https://doi.org/10.1016/j.atmosenv.2015.02.006

Chen, G. C., Tam, N. F. Y., & Ye, Y. (2010). Summer fluxes of atmospheric greenhouse gases N_2O, CH_4 and CO_2 from mangrove soil in South China. *Science of the Total Environment*, *408*(13), 2761–2767. https://doi.org/10.1016/j.scitotenv.2010.03.007

Chen, G. C., Tam, N. F., & Ye, Y. (2012). Spatial and seasonal variations of atmospheric N_2O and CO_2 fluxes from a subtropical mangrove swamp and their relationships with soil characteristics. *Soil Biology and Biochemistry*, *48*, 175–181. https://doi.org/10.1016/j.soilbio.2012.01.029

Chen, G. C., Ulumuddin, Y. I., Pramudji, S., Chen, S. Y., Chen, B., Ye, Y., Ou, D. Y., Ma, Z. Y., Hao, H., & Wang, J. K. (2014). Rich soil carbon and nitrogen but low atmospheric greenhouse gas fluxes from North Sulawesi mangrove swamps in Indonesia. *Science of the Total Environment*, *487*, 91–96. https://doi.org/10.1016/j.scitotenv.2014.03.140

Chen, G., Chen, B., Yu, D., Tam, N. F., Ye, Y., & Chen, S. (2016). Soil greenhouse gas emissions reduce the contribution of mangrove plants to the atmospheric cooling effect. *Environmental Research Letters*, *11*(12), 124019. https://doi.org/10.1088/1748-9326/11/12/124019

Dalmagro, H. J., Zanella de Arruda, P. H., Vourlitis, G. L., Lathuillière, M. J., de S. Nogueira, J., Couto, E. G., & Johnson, M. S. (2019). Radiative forcing of methane fluxes offsets net carbon dioxide uptake for a tropical flooded forest. *Global Change Biology*, *25*(6), 1967–1981. https://doi.org/10.1111/gcb.14615

Dharmawan, I.W.E., Suyarso, Ulumuddin Y.I., Prayudha B., & Pramudji. (2020). *Manual for mangrove community structure monitoring and research in Indonesia*. NAS Media Pustaka, Makassar. Retreived from: https://www.researchgate.net/publication/364326020

Denpasar Central Statistics Agency. (2022). *Denpasar municipality in figures* (pp. 243). BPS Kota Denpasar. https://denpasarkota.bps.go.id/publication/2022/02/25/68f4c38625094b798b0471a6/kota-denpasar-dalam-angka-2022.html

Dermawan, E. P., Siregar, Y. I., & Efriyeldi, E. (2023). Estimation of carbon reserves in sediments in the mangrove ecosystem of Bukit Batu Village, Bengkalis Regency, Riau. *Asian Journal of Aquatic Sciences*, *6*(1), 93–101. https://garuda.kemdikbud.go.id/documents/detail/3418183.

Dharmawan, I. W. E., & Ulumuddin Y. I. (2021). *Mangrove community structure data analysis, a guidebook for Mangrove Health Index (MHI) training* (pp. 29). NAS Media Pustaka. https://www.researchgate.net/publication/352932003_Mangrove_Community_Structure_Data_Analysis_A_Guidebook_for_Mangrove_Health_Index_MHI_Training

Fernandes, S. O., Bharathi, P. L., Bonin, P. C., & Michotey, V. D. (2010). Denitrification: An important pathway for nitrous oxide production in tropical mangrove sediments (Goa, India). *Journal of Environmental Quality*, *39*(4), 1507–1516. https://doi.org/10.2134/jeq2009.0477

Giesen, W., Wulffraat, S., Zieren, M., & Scholten, L. (2007). *Mangrove guidebook for Southeast Asia* (pp. 769). FAO and Wetlands International. https://www.fao.org/3/ag132e/ag132e00.pdf

Hirota, M., Senga, Y., Seike, Y., Nohara, S., & Kunii, H. (2007). Fluxes of carbon dioxide, methane and nitrous oxide in two contrastive fringing zones of coastal lagoon, Lake Nakaumi, Japan. *Chemosphere*, *68*(3), 597–603. https://doi.org/10.1016/j.chemosphere.2007.01.002

Imamsyah, A., Bengen, D. G., & Ismet, M. S. (2020). Structure and distribution of mangrove vegetation based on the quality of the biophysical environment in the Ngurah Rai Grand Forest Park, Bali [Indonesian]. *Ecotrophic*, *14*(1), 88–99. https://doi.org/10.24843/EJES.2020.v14.i01.p08

IPCC. (2021). *Climate change 2021: The physical science basis* (p. 2391). Contribution of Working Group I to the Sixth Assessment Report of the Intergovernmental Panel on Climate Change [Masson-Delmotte, V., P. Zhai, A. Pirani, S.L. Connors, C. Péan, S. Berger, N. Caud, Y. Chen, L. Goldfarb, M.I. Gomis, M. Huang, K. Leitzell, E. Lonnoy, J.B.R. Matthews, T.K. Maycock, T. Waterfield, O. Yelekçi, R. Yu, and B. Zhou (eds.)]. Cambridge University Press. https://doi.org/10.1017/9781009157896

Ishida, M. (2004). Automatic thresholding for digital hemispherical photography. *Canadian Journal of Forest Research*, *34*(11), 2208–2216. https://doi.org/10.1139/X04-103

Jennings, S. B., Brown, N. D., & Sheil, D. (1999). Assessing forest canopies and understorey illumination: Canopy closure, canopy cover and other measures. *Forestry: An International Journal of Forest Research*, *72*(1), 59–74. https://doi.org/10.1093/forestry/72.1.59

Kauffman, J.B., & Donato, D. C. (2012). *Protocols for the measurement, monitoring and reporting of structure, biomass and carbon stocks in mangrove forests (Vol. 86)*. Cifor. Retreived from https://www.cifor.org/publications/pdf_files/WPapers/WP86CIFOR.pdf

Kitpakornsanti, K., Pengthamkeerati, P., Limsakul, A., Worachananant, P., & Diloksumpun, S. (2022). Greenhouse gas emissions from soil and water surface in different mangrove establishments and management in Ranong Biosphere Reserve, Thailand. *Regional Studies in Marine Science*, *56*, 102690. https://doi.org/10.1016/j.rsma.2022.102690

Kristensen, E., Flindt, M. R., Ulomi, S., Borges, A. V., Abril, G., & Bouillon, S. (2008). Emission of CO_2 and CH_4 to the atmosphere by sediments and open waters in two Tanzanian mangrove forests. *Marine Ecology Progress Series*, *370*, 53–67. https://doi.org/10.3354/meps07642

Kweku, D. W., Bismark, O., Maxwell, A., Desmond, K. A., Danso, K. B., Oti-Mensah, E. A., Quachie, T., & Adormaa, B. B. (2018). Greenhouse effect: Greenhouse gases and their impact on global warming. *Journal of Scientific Research and Reports*, *17*(6), 1–9. https://doi.org/10.9734/JSRR/2017/39630

Li, N., Chen, P., & Qin, C. (2015). Density, storage and distribution of carbon in mangrove ecosystem in Guangdong's coastal areas. *Asian Agricultural Research*, *7*(1812-2016–144390), 62–73. https://doi.org/10.22004/ag.econ.202107

Lin, C. W., Kao, Y. C., Chou, M. C., Wu, H. H., Ho, C. W., & Lin, H. J. (2020). Methane emissions from subtropical and tropical mangrove ecosystems in Taiwan. *Forests*, *11*(4), 470. https://doi.org/10.3390/f11040470

LIPI. (2018). *Potential reserves of carbon absorption in mangrove and seagrass ecosystems in Indonesia*. Indonesian Institute of Sciences. Retrieved from http://oseanografi.lipi.go.id/haspen/01.%20Summary%20for%20policy%20maker-layout-20%20Juli-versi%20alfa%201.0%20release.pdf

Lugo, A. E., & Snedaker, S. C. (1974). The ecology of mangroves. *Annual Review of Ecology and Systematics*, *51*(1), 39–64. http://www2.agroparistech.fr/geeft/Downloads/Training/TropEcol/Archives_2011/4.1a.pdf.

Lu, C.Y., Wong, Y.S., Tam, N.F., Ye, Y., & Lin, P. (1999). Methane flux and production from sediments of a mangrove wetland on Hainan Island, China. *Mangroves and Salt Marshes, 3*(1): 41–49. https://doi.org/10.1023/A:1009989026801

Maiti, S. K., & Chowdhury, A. (2013). Effects of anthropogenic pollution on mangrove biodiversity: A review. *Journal of Environmental Protection*, *4*(12), 1428–1434. https://doi.org/10.4236/jep.2013.412163

Maltby, J., Sommer, S., Dale, A. W., & Treude, T. (2016). Microbial methanogenesis in the sulfate-reducing zone of surface sediments traversing the Peruvian margin. *Biogeosciences*, *13*(1), 283–299. https://doi.org/10.5194/bg-13-283-2016

Marton, J. M., Herbert, E. R., & Craft, C. B. (2012). Effects of salinity on denitrification and greenhouse gas production from laboratory-incubated tidal forest soils. *Wetlands*, *32*, 347–357. https://doi.org/10.1007/s13157-012-0270-3

Montzka, S. A., Dlugokencky, E. J., & Butler, J. H. (2011). Non-CO_2 greenhouse gases and climate change. *Nature*, *476*(7358), 43–50. https://doi.org/10.1038/nature10322

Morell, F. J., Cantero-Martínez, C., Lampurlanés, J., Plaza-Bonilla, D., & Álvaro-Fuentes, J. (2011). Soil carbon dioxide flux and organic carbon content: Effects of tillage and nitrogen fertilization. *Soil Science Society of America Journal*, *75*(5), 1874–1884. https://doi.org/10.2136/sssaj2011.0030

Murdiyarso, D., Purbopuspito, J., Kauffman, J. B., Warren, M. W., Sasmito, S. D., Donato, D. C., Manuri, S., Krisnawati, H., Tiberima, S., & Kurnianto, S. (2015). The potential of Indonesian mangrove forests for global climate change mitigation. *Nature Climate Change*, *5*(12), 1089–1092. https://doi.org/10.1038/nclimate2734

Naidoo, G. (2016). The mangroves of South Africa: An ecophysiological review. *South African Journal of Botany*, *107*, 101–113. https://doi.org/10.1016/j.sajb.2016.04.014

Otero, X. L., Araújo, J. M., Jr., Barcellos, D., Queiroz, H. M., Romero, D. J., Nóbrega, G. N., Neto, M. S., & Ferreira, T. O. (2020). Crab bioturbation and seasonality control nitrous oxide emissions in semiarid mangrove forests (Ceará, Brazil). *Applied Sciences*, *10*(7), 2215. https://doi.org/10.3390/app10072215

Philipp, K., Juang, J.-Y., Deventer, M. J., & Klemm, O. (2017). Methane emissions from a subtropical grass marshland, northern Taiwan. *Wetlands*, *37*(6), 1145–1157. https://doi.org/10.1007/s13157-017-0947-8

Pillai, N. G., & Harilal, C. C. (2016). Surveillance of the tolerance limit of Sonnearia alba Sm. to certain hydrogeochemical parameters from heterogenous natural habitats of Kerala, South India. *International Research Journal of Biological Sciences*, *5*(12), 28–37. https://www.researchgate.net/publication/311616208.

Prinasti, N. K. D., Dharma, I. G. B. S., & Suteja, Y. (2020). Community structure of mangrove vegetation based on substrate characteristics in Ngurah Rai Forest Park, Bali [Indonesian]. *Journal of Marine and Aquatic Sciences*, *6*(1), 90–99. https://doi.org/10.24843/jmas.2020.v06.i01.p11

Purvaja, R., & Ramesh, R. (2001). Natural and anthropogenic methane emission from coastal wetlands of South India. *Environmental Management*, *27*(4), 547–557. https://doi.org/10.1007/s002670010169

Queiroz, H. M., Artur, A. G., Taniguchi, C. A. K., da Silveira, M. R. S., do Nascimento, J. C., Nóbrega, G. N., Otero, X. L., & Ferreira, T. O. (2019). Hidden contribution of shrimp farming effluents to greenhouse gas emissions from mangrove soils. *Estuarine, Coastal and Shelf Science*, *221*, 8–14. https://doi.org/10.1016/j.ecss.2019.03.011

Raharja, I. M. D., Hendrawana, I. G., & Suteja, Y. (2018). Modeling of nitrate distribution in the waters of Benoa Bay [Indonesian]. *Journal of Marine Research and Technology*, *1*(1), 22–28. https://doi.org/10.24843/jmrt.2018.v01.i01.p05

Rahayu, N. W. S. T., Hendrawan, I. G., & Suteja, Y. (2018). Spatial and temporal distribution of nitrate and phosphate during the western monsoon on the surface of Benoa Bay, Bali [Indonesian]. *Journal of Marine and Aquatic Sciences*, *4*(1), 1–13. https://doi.org/10.24843/jmas.2018.v4.i01.1-13

Reay, D. S., Smith, P., Christensen, T. R., James, R. H., & Clark, H. (2018). Methane and global environmental change. *Annual Review of Environment and Resources*, *43*, 165–192. https://doi.org/10.1146/annurev-environ-102017-030154

Richards, D. R., & Friess, D. A. (2016). Rates and drivers of mangrove deforestation in Southeast Asia, 2000–2012. *Proceedings of the National Academy of Sciences*, *113*(2), 344–349. https://doi.org/10.1073/pnas.1510272113

Rosentreter, J. A., Al-Haj, A. N., Fulweiler, R. W., & Williamson, P. (2021). Methane and nitrous oxide emissions complicate coastal blue carbon assessments. *Global Biogeochemical Cycles*, *35*(2), e2020GB006858. https://doi.org/10.1029/2020GB006858

Sánchez-Carrillo, S., Garatuza-Payan, J., Sánchez-Andrés, R., Cervantes, F. J., Bartolomé, M. C., Merino-Ibarra, M., & Thalasso, F. (2021). Methane production and oxidation in mangrove soils assessed by stable isotope mass balances. *Water*, *13*(13), 1867. https://doi.org/10.3390/w13131867

Sasmito, S. D., Taillardat, P., Clendenning, J. N., Cameron, C., Friess, D. A., Murdiyarso, D., & Hutley, L. B. (2019). Effect of land-use and land-cover change on mangrove blue carbon: A systematic review. *Global Change Biology*, *25*(12), 4291–4302. https://doi.org/10.1111/gcb.14774

Shiau, Y. J., & Chiu, C. Y. (2020). Biogeochemical processes of C and N in the soil of mangrove forest ecosystems. *Forests*, *11*(5), 492. https://doi.org/10.3390/f11050492

Shih, S. S., & Cheng, T. Y. (2022). Geomorphological dynamics of tidal channels and flats in mangrove swamps. *Estuarine, Coastal and Shelf Science*, *265*, 107704. https://doi.org/10.1016/j.ecss.2021.107704

Sidik, F., Fernanda Adame, M., & Lovelock, C. E. (2019). Carbon sequestration and fluxes of restored mangroves in abandoned aquaculture ponds. *Journal of the Indian Ocean Region*, *15*(2), 177–192. https://doi.org/10.1080/19480881.2019.1605659

Srikanth, S., Lum, S. K. Y., & Chen, Z. (2016). Mangrove root: Adaptations and ecological importance. *Trees*, *30*, 451–465. https://doi.org/10.1007/s00468-015-1233-0

Sugiana, I. P., Faiqoh, E., Indrawan, G. S., & Dharmawan, I. W. E. (2021). Methane concentration on three mangrove zones in Ngurah Rai Forest Park, Bali [Indonesian]. *Jurnal Ilmu Lingkungan*, *19*(2), 422–431. https://doi.org/10.14710/jil.19.2.422-431

Sugiana, I. P., Andiani, A. A. E., Dewi, I. G. A. I. P., Karang, I. W. G. A., As-Syakur, A. R., & Dharmawan, I. W. E. (2022). Spatial distribution of mangrove health index on three genera dominated zones in Benoa Bay, Bali, Indonesia. *Biodiversitas Journal of Biological Diversity*, *23*(7). https://doi.org/10.13057/biodiv/d230713

Tang, A. C., Stoy, P. C., Hirata, R., Musin, K. K., Aeries, E. B., Wenceslaus, J., & Melling, L. (2018). Eddy covariance measurements of methane flux at a tropical peat forest in Sarawak, Malaysian Borneo. *Geophysical Research Letters*, *45*(9), 4390–4399. https://doi.org/10.1029/2017GL076457

Tomlinson, P. (2016). *The botany of mangroves* (2nd ed., p. 418). Cambridge University Press. https://doi.org/10.1017/CBO9781139946575

Treat, C. C., Natali, S. M., Ernakovich, J., Iversen, C. M., Lupascu, M., McGuire, A. D., Norby, R. J., Chowdhury, R., Richter, A., Šantrůčková, H., & Waldrop, M. P. (2015). A pan-Arctic synthesis of CH_4 and CO_2 production from anoxic soil incubations. *Global Change Biology*, *21*(7), 2787–2803. https://doi.org/10.1111/gcb.12875

Ulumuddin, Y. I. (2019). Methane: Greenhouse gas emissions from blue carbon ecosystems, mangroves [Indonesian]. *Jurnal Ilmu Lingkungan*, *17*(2), 359–372. https://doi.org/10.14710/jil.17.2.359-372

Wang, D., Chen, Z., Sun, W., Hu, B., & Xu, S. (2009). Methane and nitrous oxide concentration and emission flux of Yangtze Delta plain river net. *Science in China Series B: Chemistry*, *52*(5), 652–661. https://doi.org/10.1007/s11426-009-0024-0

Weiss, C., Weiss, J., Boy, J., Iskandar, I., Mikutta, R., & Guggenberger, G. (2016). Soil organic carbon stocks in estuarine and marine mangrove ecosystems are driven by nutrient colimitation of P and N. *Ecology and Evolution*, *6*(14), 5043–5056. https://doi.org/10.1002/ece3.2258

Welti, N., Hayes, M., & Lockington, D. (2017). Seasonal nitrous oxide and methane emissions across a subtropical estuarine salinity gradient. *Biogeochemistry, 132*(1), 55–69. https://doi.org/10.1007/s10533-016-0287-4

Wentworth, C. K. (1922). A scale of grade and class terms for clastic sediments. *The Journal of Geology*, *30*(5), 377–392. https://www.journals.uchicago.edu/doi/pdf/10.1086/622910.

Zhang, Y., Liang, F. P., Li, Y. Y. W., Zhang, J. W., Zhang, S. J., Bai, H., Liu, Q., Zhong, C. Y. R., & Li, L. (2018). Allelopathic effects of leachates from two alien mangrove species, Sonneratia apetala and Laguncularia racemosa on seed germination, seedling growth and antioxidative activity of a native mangrove species Sonneratia caseolaris. *Allelopathy Journal*, *44*(1), 119–130. https://www.researchgate.net/publication/333262758.

Zhu, X., Burger, M., Doane, T. A., & Horwath, W. R. (2013). Ammonia oxidation pathways and nitrifier denitrification are significant sources of N_2O and NO under low oxygen availability. *Proceedings of the National Academy of Sciences*, *110*(16), 6328–6333. https://doi.org/10.1073/pnas.1219993110

Zhu, X., Sun, C., & Qin, Z. (2021). Drought-induced salinity enhancement weakens mangrove greenhouse gas cycling. *Journal of Geophysical Research: Biogeosciences*, *126*(8), e2021JG006416. https://doi.org/10.1029/2021JG006416

Publisher's Note

Springer Nature remains neutral with regard to jurisdictional claims in published maps and institutional affiliations.